Active Control of a Flexible Rotor by an Active Bearing

Yoichi KANEMITSU, Masaru OHSAWA, Katsuhide WATANABE

EBARA RESEARCH Co.,LTD.
4-2-1 Honfujisawa,Fujisawa-shi,251,JAPAN

SUMMARY

This paper details the effects of analog and digital compensation circuits used when passing through critical speeds of a flexible rotor suspended by an active magnetic bearing. Several kinds of filters are used for rotation tests and vibration characteristics of the rotor are measured. A digital IIR filter implemented by a DSP could attenuate the vibration of the rotor at critical speeds.

INTRODUCTION

A magnetic bearing which uses DC magnets consists of proximity sensors measuring relative diplacement between rotor and stator, electric circuits regulating current to keep input signal from proximity sensor constant and DC electlic magnets as actuator.

We have made a five axis active magnetic bearing as an experiment and controlled it by using an analog circuit, a digital FIR filter circuit and a digital IIR filter circuit as a compensator in order to support a flexible rotor. A digital compensator is suitable for adaptive or optimal control because the properties of the compensator can be easily changed by modifying it's software. The validity of these circuits is confirmed by rotation tests of the rotor operating beyond the bending natural frequencies of rotor.

MAGNETIC PULL OF RADIAL POLE

A radial magnetic bearing(RMB) has 4 electric magnets as shown in FIg.1. The magnetic pull between the rotor and stator is calculated from the magnetic flux density in the clearance between the rotor and stator and also the magnetic flux density excited by the stator pole coil is calculated by the permeance method based on the ralation between magnet-motive force IN and magnetic intensity H in each magnetic pole given by Ampere's law.

Fig.2 shows a comparison of the relations between magnetmotive force, gap and magnetic pull calculated by the permeance method and by a 2-dimensional magnetic field analysis using the finite element method. In this figure, magnetic pull by the permeance method becomes large as the magnetmotive force increases and saturates near 600N. The value from FEM is slightly smaller than that calculated by the permeance method because leakage flux must take place and be neglected in the permeance method.

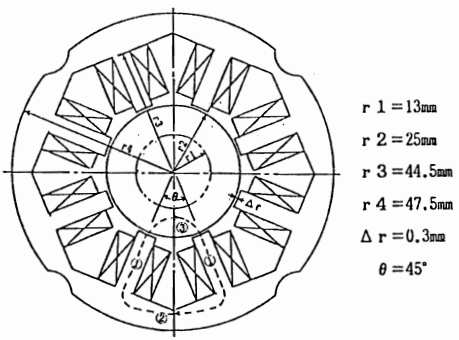

Fig.1 Shape of Radial Magnetic Bearing

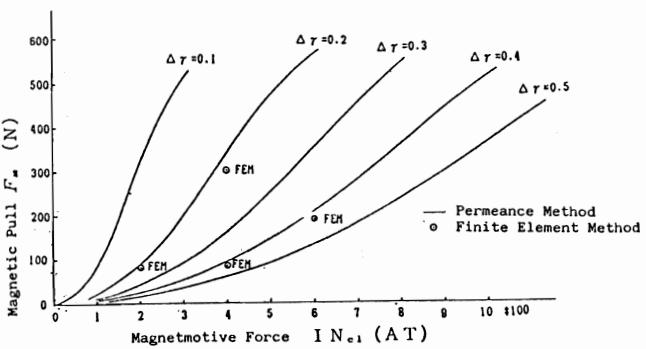

Fig.2 Magnetic Pull of Radial Magnetic Bearing

CONFIGRATION OF CONTROLLER

Each axis of the active magnetic bearing(AMB) is regulated individually and it's controller is made up of a shift circuit of a displacement signal, a compensation circuit, two driver and two power amplifiers. The block diagram of the system is shown in Fig.3. The shift circuit of the displacement signal corrects an error of signal and retains the rotor at the desired position. The compensation circuit is made up of a integration circuit to increase static rigidity, a phase lead circuit to increase damping force of the rotor in the frequency range above rigid mode

natural frequency and a low pass filter to attenuate the gain in high frequency.

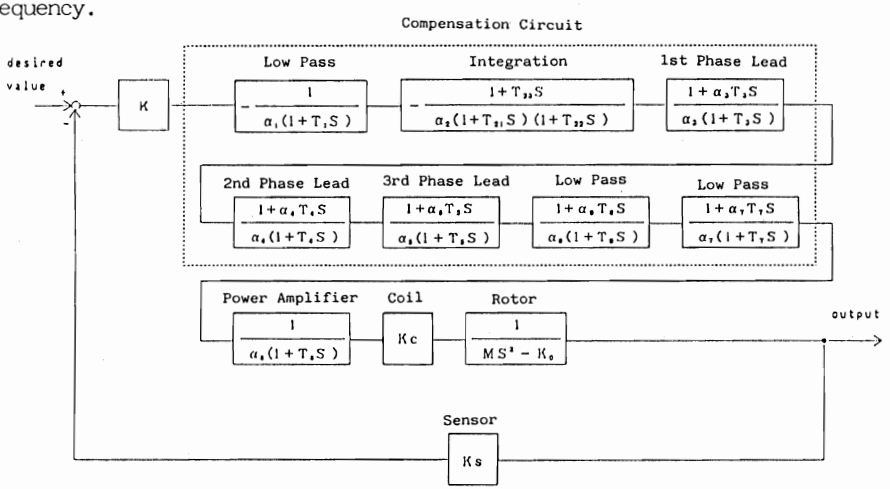

Fig.3 Block Diagram of System

TEST APPARATUS

Fig.4 shows a test apparatus for attesting the ability of the analog compensator and digital compensator. The shaft is 531mm in length, and 26mm in maximum diameter. A motor rotor is located in the middle of the shaft and two RMB rotors are situated on both sides of the motor rotor. A thrust magnetic bearing(TMB) is located at left end of shaft. Eddy current type proximity sensors with two mounting holes are prepared for the RMB sensors at both sides of the bearing.

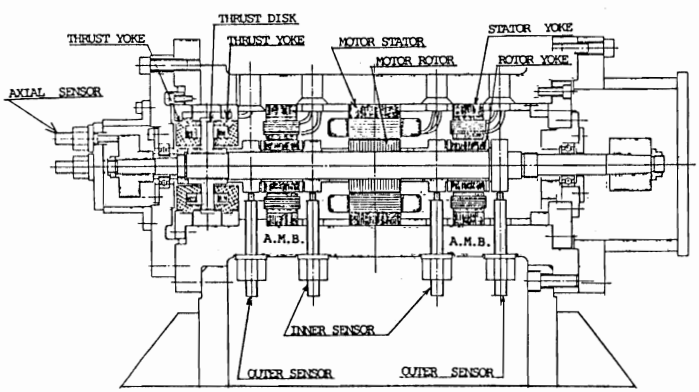

Fig.4 Test Apparatus

The natural frequencies and modes of the test rotor measured in a free-free state are presented in Fig.5. According to this figure the outer sensor of the left bearing coincided with a nodal point of 1st mode so that the observability of this mode cannot be achieved by this sensor.

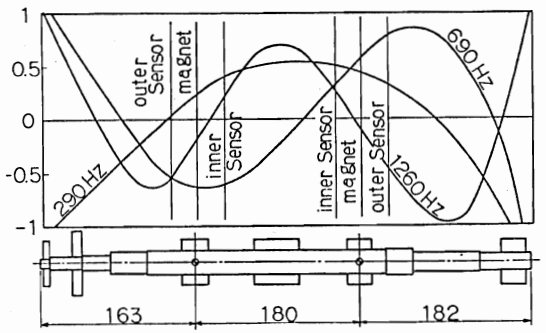

Fig.5 Natural Vibration Modes of Rotor

VIBRATION DURING ROTATION TEST WITH ANALOG COMPENSATOR

For an analog compensator, a compensation circuit(A) containing a low-pass filter at high-frequencies and ones(B) without it were made and their measured transfer functions are as shown in Fig.6. Design of the compensation circuit without a low pass filter was based on the idea that the gain at high frequencies would be reduced by the mass effect of the rotor to be controlled and that it would be better in the interest of stability to advance the phase up to the highest frequency possible.

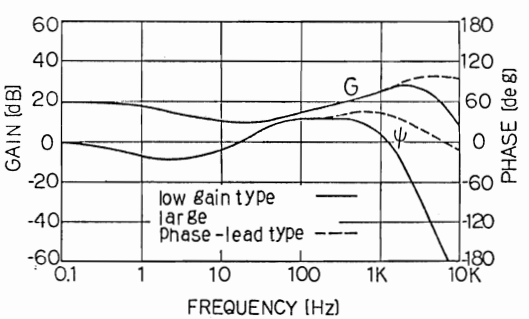

Fig.6 Transfer Fanction of Analog Compensator

Fig.7 and Fig.8 show waterfall diagrams of displacement vibration using the inner sensors at the inner proximity sensor. When the outer sensors were used, unstable vibration occured near the first critical speed and the rotating speed could not be increased.

Fig.7 is the test result using the inner sensor and the analog compensator(A). Here the rotor reached 32,000rpm, but 1st natural vibration occured at this speed.

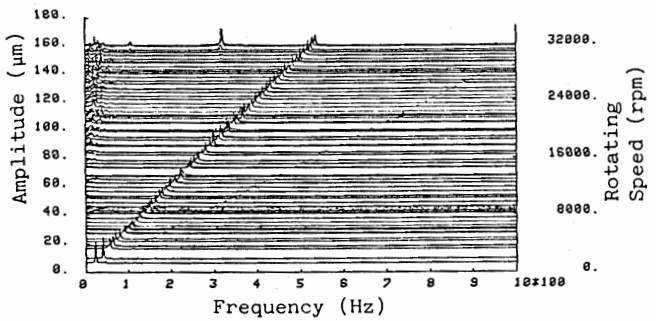

Fig.7 Radial Vibration of Rotor with Compensator(A)

Next, Fig.8 shows results of a rotating test using the compensator(B) which has a larger phase-lead than compensator(A) as shown in Fig.6. The rotating speed reached 40,000rpm by compensator(B) without unstable vibration because of the increase in phase-lead. Maximum rotating speed in a series of rotating tests using the inner sensor is 40,000rpm which is just below the second critical speed of 42,000rpm. As each test has no rigid mode resonance, and small resonance of 1st bending mode, we proved that the analog compensator has sufficient damping action in these frequency ranges. But this compensator could not give the rotor sufficient

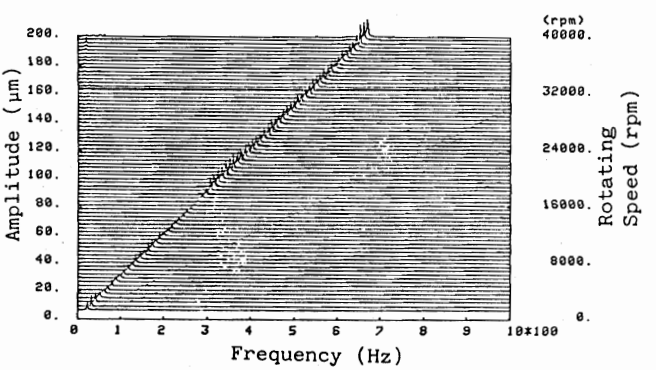

Fig.8 Radial Vibration of Rotor with Compensator(B)

damping force to suppress the 2nd natural frequency, so that the rotor vibration became larger near this natural frequency. The DN value of radial AMB is about 2×10^6 and it's circumferential velocity is 104m/s, which is faster than that of a conventional bearing.

CONTROL BY DIGITAL FIR COMPENSATOR

Using the transfer function of compensator H(s), we get the impulse response of compensator h(t) as follows.

$$h(t)=\frac{1}{2\pi}\int_{-\infty}^{\infty}H(j\omega)\,e^{j\omega t}\,d\omega \qquad \text{——— (1)}$$

The output y(t) is obtained by following convolution integral because the system responds to the past input alone.

$$y(t)=\int_{0}^{\infty}h(\tau)\,x(t-\tau)\,d\tau \qquad \text{——— (2)}$$

Where x(t) is input. In discrete system of which sampling period is Δt, y(t), h(t), and x(t) are expressed as y(n), h(n), x(n) at $n\cdot\Delta t$ respectively. Eq(2) can be described as follows.

$$y(n)=\sum_{p=0}^{\infty}h(p)\,x(n-p) \qquad \text{——— (3)}$$

The impulse response of a real filter converges within finite time, so that we substitute as follows.

$$h(p)=0 \quad (p>m) \qquad \text{——— (4)}$$

A FIR compensator of 128 taps (m=127) requres 128 times multiplication, addition and memory access. In order to calculate this FIR compensator by a general purpose MPU(micro processing unit) such as Z80, A 2-byte addition needs 135 cycles and A 2-byte multiplication needs 327 cycles. When frequency of clock is 6MHz, the sampling period is 1/101 { $=128\times(135+327)/6\times10^6$ }. Because sampling frequency of system with a general MPU would be almost 100Hz even if time of access to memory was ignored, a MPU is unsuitable for controlling a high speed AMB. For that reason, we used a 16×16 bits multiplier-accumulator NPC/SM5810-BD(pin-compatible with TRW/TDC1010J) which is able to calculate multiplication and addition within 65ns. Time for calculation of the FIR compensator with SM5810BD is as follows.

(1) A/D conversion (DATEL ADC-HS12) 15μs

(2) reading filter coefficients(SRAM HM6116) 200ns×128=25.6μs

(3) multipliscation and accumulation 65ns×128=8.3μs

(4) imput signal shift 200ns×128=25.6μs

(5) D/A conversion (DATEL DAC – Hz12) 3μs

Total time of (1)–(5) is 77.5μs, so that sampling frequency can be raised to 12kHz and this filter may be applied to an AMB. We put the desired transfer function of the compensator into a personal computer and obtained the impulse response of the compensator by the inverse fast fourier transform. Time series datum of impulse response is equivalent to the coefficients of the FIR compensator. After these coefficients are sent to memory in the FIR compensator board from the host computer, the FIR compensator begins to regulate rotor motion.

Fig.9 shows the block diagram of hardware for the FIR compensator.

For the purpose of testing the FIR compensator hardwere, we replaced coefficients by

$$h(i)=1 \quad (i=0)$$
$$=0 \quad (i=1\text{-}127) \qquad \text{——— (5)}$$

and measured the FIR compensator property. When the system clock frequency is chosen at 2MHz, the sampling frequency results in 7812Hz.

Fig.10 shows the measured transfer function of the FIR compensator with 7812Hz in the sampling frequency. The characteristics of gain G(f) are flat up to 4kHZ, but the phase becomes -2π at 3906Hz which is Nyquist frequency. Therefore we may conclude that this hardware has a sufficient function.

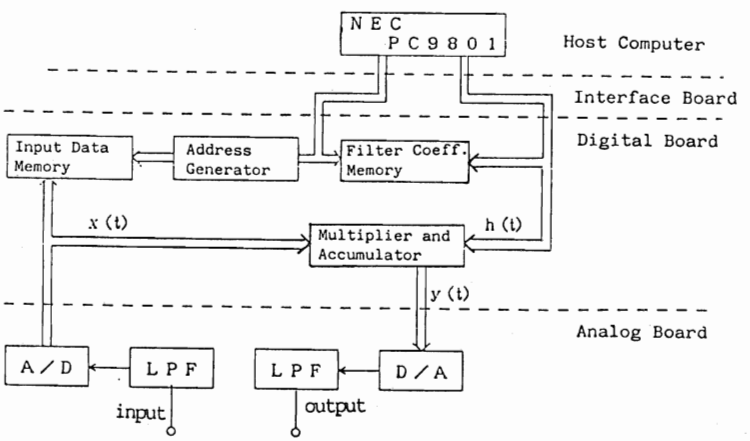

Fig.9 Block Diagram of FIR Filter Compensator

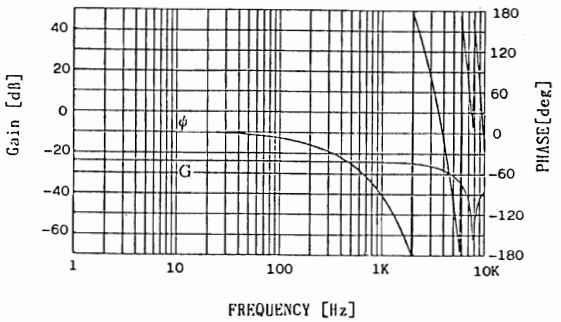

Fig.10 Measured Transfer Function of FIR Filter (Flat)

As the PID filter is considered as a type of FIR filter, PID control for AMB is feasible with the hardware shown in Fig.9. Firstly this compensation circuit is applied to control of axial direction. The filter coefficient was set so as to attain a phase lead of 45° at 130Hz where a resonance frequency of the axial direction is present. The transfer function of PID type and PD type filters are shown in Fig.11.

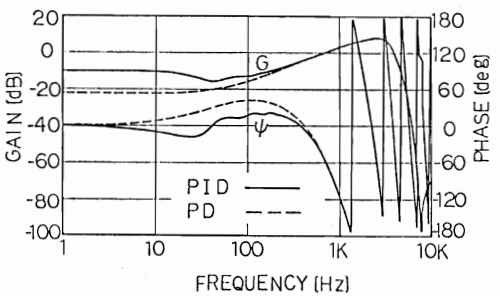

Fig.11 FIR Filter Characteristics

When a PID filter was used as a compensation circuit, low frequency vibration occured. The phase-lag of 5-40Hz of the filter was thought to be the cause of these vibration and the coefficients were changed to a PD type filter to advance the phase in this frequency region. The results of rotation tests using this filter for axial direction control are shown in Fig.12.

In this test the critical speed in the axial direction was 5,000rpm and vibration of 20 μm was observed there. After the critical speed the

vibration was reduced to 10 μm or so and the speed was increased to 30,000rpm.

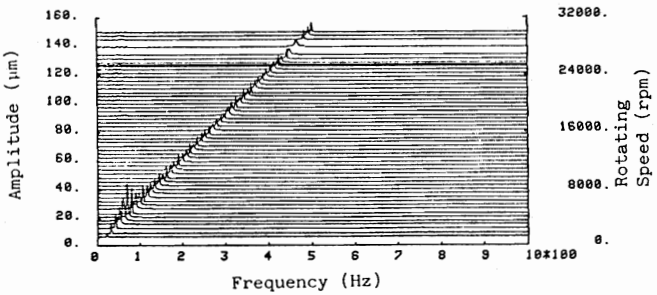

Fig.12 Axial Direction Control by FIR Compensator(PD)

Next this filter was installed in place of an analog compensation in the horizontal direction of a RMB on the free end and a rotation test was carried out. The results are shown in Fig.13. Vibration of 30μm or so was only observed near the critical speed of 2,000rpm in the rigid mode and the speed could be increased in small amplitudes up to near the 1st bending critical speed of 18,000rpm. As the speed approached this critical speed, synchronous vibration increased abruptly so that it was impossible to increase the speed beyond this critical speed, because almost no phase lead took place in the frequency region near 300Hz in Fig.11.

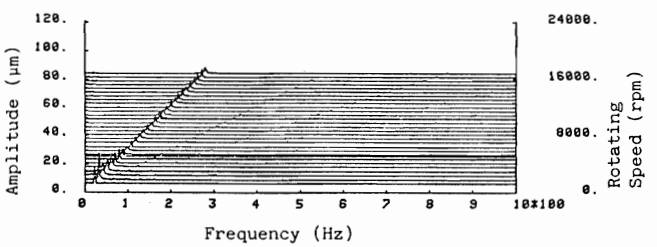

Fig.13 Radial Control with Fir Compensator(PD)

CONTROL USING DIGITAL COMPENSATOR WITH DSP

Based on an analog compensator where the speed was raised beyond the 1st bending natural frequency of the rotor, an IIR filter compensator was prepared. The analog compensator must have parts changed when it is necessary to change their filter characteristics. With digital compensators, their filter characteristics are altered by changing the contents of

the filter coefficient memory. Therefore, if it is possible to change the memory contents during operation, an optimal or adaptive control may be realized. As the first step toward this objective, an IIR filter based on a known analog compensator was prepared. When the transfer fanction G(s) on s-plane is given, the transfer function D(z) on z-plane is found by bilinear transformation expressed below

$$D(z)=G(s)\Big|_{s=\frac{2}{T}\cdot\frac{1-Z^{-1}}{1+Z^{-1}}} \qquad \text{——— (6)}$$

Where T is the sampling period. As the relation between input X(z) and output Y(z) of the n stages second-order IIR filter can be expressed as follows,

$$\frac{Y(z)}{X(z)} = D(z)=\prod^{n}\frac{U(z)}{E(z)} =\prod^{n}\frac{b_0+b_1Z^{-1}+b_2Z^{-2}}{1+a_1Z^{-1}+a_2Z^{-2}} \qquad \text{— (7)}$$

the filter output Y(z) can be found by calculating the output of each stage sequentially. The output u(n) of each stage at t=n·T is found as follows.

$$u(n) = b_0\ e(n) + b_1\ e(n-1) + b_2\ e(n-2) - a_1\ u(n-1) - a_2\ u(n-2) \qquad \text{——— (8)}$$

With the FIR filters a high-speed multiplier and accumulator SM5810 was used for high speed repetition of simple multiplication and addition. But with the IIR filter, the number of multiplication and additions performed is fewer than with the FIR filter, and the handling of numerical values is more complicated. As a result, a digital signal processor TI/TMS320C25 is used. With this DSP, a high-speed A/D converter(DATEL ADC817) and 3 D/A converters were used to make 3 compensators consisting of 7 stages 2nd-order IIR filters. At the sampling frequency of 4000Hz for each axis (12kHz in total), it operated at an instruction time of 125ns. Up to 665 instructions can be executed during this sampling interval. Actually 366 instructions were necessary to operate this filter, whose block diagram is shown in Fig.14. The AMB system with this filter shown in Fig.15 converts analog signals from the sensor to digital signals and stores them in the IIR filter. It also changes the compensated digital signals to analog signal for output.

A comparison between the transfer function of the analog and digital filters is shown in Fig.16. The IIR filter(1) is designed to have the same properties as the analog filter and the IIR filter(2) has an additional

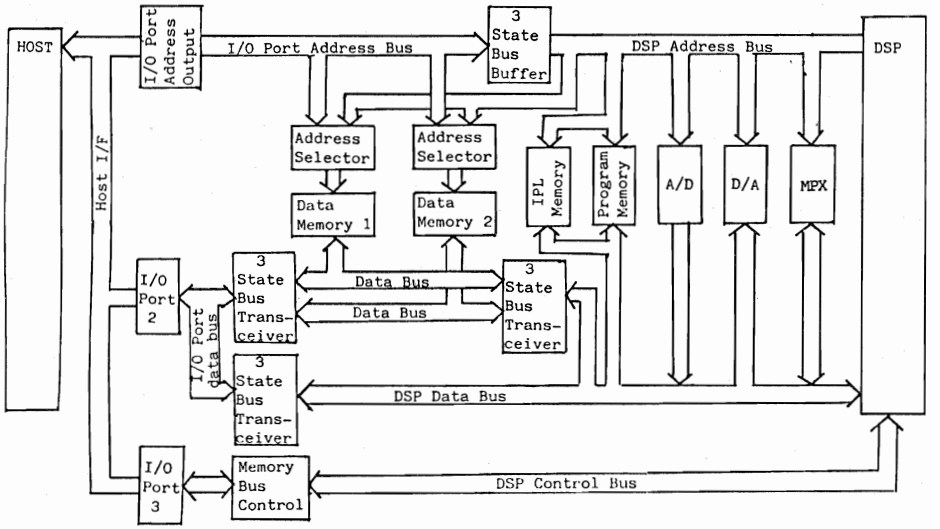

Fig.14 IIR Filter Block Diagram

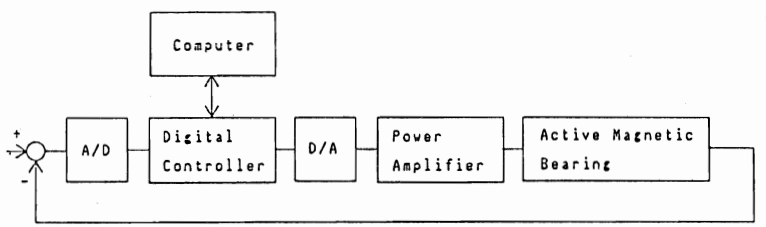

Fig.15 Digital Control Systm

second-order phase lag-lead stage. The gain G of the IIR filter(1) agrees with the gain of the analog filter up to 70OHz. Beyond this frequency, however, the gain of the IIR filter(1) increases and falls abruptly beyond a certain frequency. A comparison of the phase reveals an agreement below 70Hz. But the phase of the IIR filter(1) begins to delay gradually beyond 70Hz. At 1kHz it delays 50° from the analog filter. With the IIR filter(1) the phase is negative above 800Hz. Especially the phase lead is 25° or so at the 1st bending natural frequency of 300Hz. Thus it is smaller than the control design target of more than 30°.

In order to attain an adequate phase lead at the natural frequencies of 300Hz and 700Hz, another IIR filter(2) was made by adding a 2nd-order phase lag-lead stage to IIR filter(1). This filter attained phase leads of about 50° and 35° at the 1st and 2nd natural frequencies of 300Hz and 700Hz. However, this modification enlarged the phase lag in the low frequency region. A waterfall diagram of radial vibration in the rotation test using IIR filters is shown in Fig.17. With the IIR filter(1), the radial vibration shown in Fig.17(a) increased near the 1st critical speed of 18,000rpm. Therefore, the speed was not increased beyond this range. With the IIR filter(2) whose phase for the frequency range including the natural frequency of the rotor is advanced sufficiently, the response charactristics were attained as showned in Fig.17(b). As a result the response is fully damped even at the critical speed. This means that the vibration of the rotor is fully controllable by means of the phase compensation. With this filter the speed was raised to 28,000rpm.

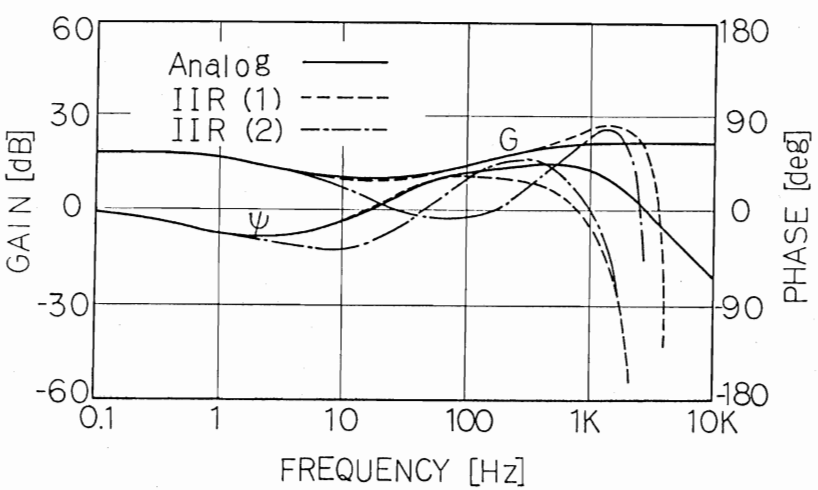

Fig.16 Comparison of Transfer Function between Analog Compensator and Digital(IIR) Compensators

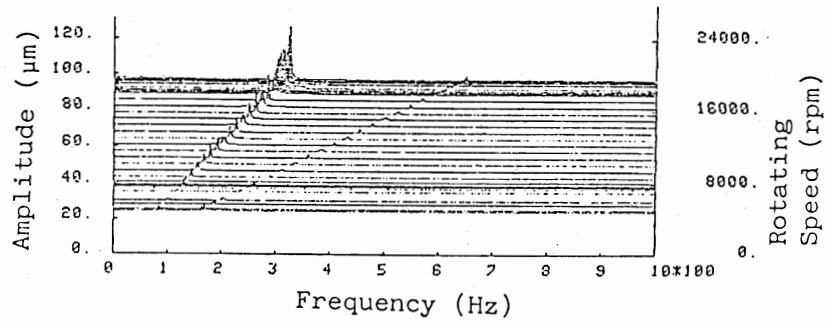

(a) In Case of IIR Filter(1)

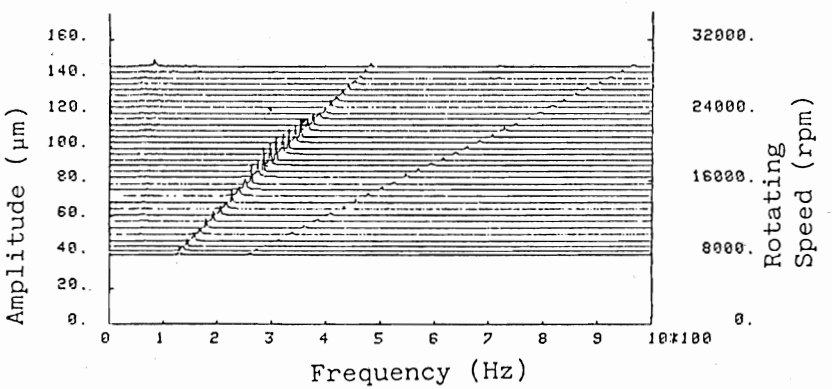

(b) In Case of IIR Filter(2)

Fig.17 Vibration in Rotor

CONCLUSION

Rotation tests were conducted by suspending the flexible rotor with the 5-axis magnetic bearing that uses DC electromagnets. With these tests analog and digital compensators were used for feedback control and vibration characteristics of the rotor were measured. Since sufficient attenuation was attained by the analog compensator, the rotor could easily pass through the 1st critical speed. The digital FIR filter was used for PD control to increase the rotor speed immediately before the first critical speed. With the digital IIR filter whose phase for the frequency range including the bending natural frequencies of rotor is advanced sufficiently, the vibration response is fully damped even at the 1st critical speed.

REFERENCES

(1) Kido,Kenichi, Introduction, to Digital Signal Processing, Maruzen (in Japanese), Tokyo, pp.183-189 (1985)

(2) Slivinsky,C., Borninski,J., Digital Signal Processing Applications with the TMS320 Family (Texas Instruments) pp.689-724 (1986)